Catalytic Performance of Bulk and Al$_2$O$_3$-Supported Molybdenum Oxide for the Production of Biodiesel from Oil with High Free Fatty Acids Content

Alberto Navajas [1,2] , **Inés Reyero** [1,2] , **Elena Jiménez-Barrera** [3], **Francisca Romero-Sarria** [3], **Jordi Llorca** [4] **and Luis M. Gandía** [1,2,*]

[1]   Departamento de Ciencias, Edificio de los Acebos, Universidad Pública de Navarra, Campus de Arrosadía s/n, 31006 Pamplona, Spain; alberto.navajas@unavarra.es (A.N.); ines.reyero@unavarra.es (I.R.)

[2]   Institute for Advanced Materials (InaMat), Universidad Pública de Navarra, Campus de Arrosadía, 31006 Pamplona, Spain

[3]   Departamento de Química Inorgánica e Instituto de Ciencia de Materiales de Sevilla, Centro mixto Universidad de Sevilla-CSIC, Av. Américo Vespucio 49, 41092 Seville, Spain; elenamaria_jb@hotmail.com (E.J.-B.); francisca@us.es (F.R.-S.)

[4]   Institute of Energy Technologies, Department of Chemical Engineering and Barcelona Research Center in Multiscale Science and Engineering. Universitat Politècnica de Catalunya, EEBE, Eduard Maristany 16, 08019 Barcelona, Spain; jordi.llorca@upc.edu

*   Correspondence: lgandia@unavarra.es

Abstract: Non-edible vegetable oils are characterized by high contents of free fatty acids (FFAs) that prevent from using the conventional basic catalysts for the production of biodiesel. In this work, solid acid catalysts are used for the simultaneous esterification and transesterification with methanol of the FFAs and triglycerides contained in sunflower oil acidified with oleic acid. Molybdenum oxide (MoO$_3$), which has been seldom considered as a catalyst for the production of biodiesel, was used in bulk and alumina-supported forms. Results showed that bulk MoO$_3$ is very active for both transesterification and esterification reactions, but it suffered from severe molybdenum leaching in the reaction medium. When supported on Al$_2$O$_3$, the MoO$_3$ performance improved in terms of active phase utilization and stability though molybdenum leaching remained significant. The improvement of catalytic performance was ascribed to the establishment of MoO$_3$-Al$_2$O$_3$ interactions that favored the anchorage of molybdenum to the support and the formation of new strong acidic centers, although this effect was offset by a decrease of specific surface area. It is concluded that the development of stable catalysts based on MoO$_3$ offers an attractive route for the valorization of oils with high FFAs content.

Keywords: acid catalysis; biodiesel; biofuel; esterification; fatty acid; methanolysis; molybdenum oxide; transesterification; vegetable oil

---

1. Introduction

Biodiesel (a mixture of fatty acid methyl esters, FAMEs) has been the most important alternative fuel for diesel engines for over 25 years [1]. It is typically produced by the catalytic transesterification of refined vegetable oils such as soybean, palm and rapeseed in liquid phase (homogeneous catalysis). To make biodiesel more cost-competitive with petroleum diesel, the use of refined oils, whose cost has been estimated to account for 70–95% of the total costs, should be avoided by replacing them with low-cost feedstocks, such as waste greases, brown grease, non-edible vegetable oils, dark oil generated by the vegetable oil refining industry, or used cooking oils [1–3]. An obvious and important additional benefit

of this strategy is obtaining a more sustainable alternative fuel that contributes to reducing the CO_2 emissions to the atmosphere and the dependency of the energy system on petroleum. On the other hand, the basic catalysts usually used in the biodiesel industry (KOH, NaOH, and potassium and sodium methoxides) have important drawbacks [4]. Although they could be replaced by heterogeneous solid catalysts to make their re-utilization possible, some issues concerning those materials such as the lack of the required chemical stability are still not well solved [5–7]. Moreover, basic catalysts are not capable of suitably processing virgin, non-edible or waste feedstocks, which are characterized by being relatively rich in free fatty acids (FFAs), because they result deactivated and/or consumed, e.g., by the formation of soaps that also complicate the separation of the products due to their emulsifying properties. In these cases, acid catalysts can be used to perform a pre-esterification of the FFAs followed by base-catalyzed transesterification giving rise to the so-called integrated process for biodiesel production from high FFAs-containing triglyceride feedstocks [1,8]. Nevertheless, this is a multistep process that introduces complexity, thus reducing the competitive advantage of using low-cost feedstocks. It would be more convenient to perform the simultaneous transformation of the triglycerides and FFAs into FAMEs, which can be in fact accomplished using heterogeneous acid catalysts [9–11].

Heterogeneous acid catalysts considered for biodiesel production comprise a large variety of materials [8–18]. The most representative ones consist on sulfated and tungstated zirconia, niobia, silica and alumina, bulk and supported polyoxometalates and heteropoly acids (HPAs) of e.g., Si^{4+} or P^{5+} with W^{6+} or Mo^{6+}, mixed metal oxides such as titania-zirconia and silica-zirconia, immobilized acidic ionic liquids, sulfonic ion-exchange resins, zeolites, mesoporous silicas (SBA, MCM and KIT series), and carbonaceous materials functionalized with sulfonic acid groups. Each of these families of compounds presents advantages and drawbacks whereas their catalytic performance is intimately related to their textural and acidic properties that depend on the exact composition, synthesis method, activation conditions, etc. In this regard, the low activity reported for zeolites has been related to the strong diffusional limitations suffered by the bulky triglyceride and FFA molecules. As for the acidic properties, Brönsted sites are considered significantly more active than the Lewis ones [10], though the necessity of having both strong Brönsted and Lewis sites has also been claimed [1]. Another typical feature of the production of biodiesel through acid catalysis is that temperatures up to around 190 °C are required to obtain reasonable product yields which is in contrast with the temperatures close to the normal boiling point of methanol (65 °C) that are employed with the basic catalysts, even the heterogeneous ones. This is obviously related to the well-known lower activity for this process of the acid catalysts compared to the basic ones.

Among the several materials proposed, sulfated zirconia (SO_4^{2-}/ZrO_2) is considered a super-acid solid exhibiting the strongest Brönsted acidity; therefore, it has been widely investigated as a catalyst for the production of biodiesel. A significant lack of stability has been reported for SO_4^{2-}/ZrO_2 due to sulfate leaching, as well as deactivation by fouling associated with surface deposition of reaction products and reactants causing the blockage of the active sites [1]. On the other hand, some compounds of tungsten and molybdenum, both metals belonging to group 6 of the Periodic Table, have been also identified as potential catalysts for the synthesis of biodiesel. Several works can be found in the literature showing the good catalytic performance of supported WO_3 for the conversion of oils with high contents of FFA [19,20]. As for molybdenum, their compounds have received little attention in this field up to date. Molybdenum compounds are characterized by a remarkable versatility as catalysts, a fact that is related to the ability of this metal to be present on the solid surface in different oxidation states, ranging from Mo^{6+} to metallic Mo (Mo^0) [21]. Anhydrous sodium molybdate [22], bulk MoO_3 [23], and molybdenum supported on alumina [24], silica, silica-alumina, and titania [25,26], as well as carbon [27] have been used as esterification and transesterification catalysts for biodiesel production from several oils, including waste oil.

In this work, both bulk (unsupported) and alumina-supported MoO_3 have been used as catalysts to convert sunflower oil with added FFAs into biodiesel. The main objective is to contribute to a better understanding of the parameters controlling the catalytic performance of these materials in pursuit

of the future development of an active, selective, and stable catalyst suitable for the production of biodiesel from non-edible and waste feedstocks.

2. Results and Discussion

2.1. Catalysts Characterization

Three bulk molybdenum oxide catalysts (Mo (300), Mo (500) and Mo (700)) were prepared through the calcination of ammonium heptamolybdate tetrahydrate (AHM) at 300, 500, and 700 °C. In addition, a series of alumina-supported molybdenum oxide catalysts (s-Mo (*x*), where *x* is the MoO_3 content (wt.%)) were obtained from the incipient wetness impregnation of alumina with aqueous AHM solutions and calcination at 800 °C.

The X-ray diffraction (XRD) patterns of the bulk and a selection of the alumina-supported molybdenum catalysts are shown in Figure 1. The thermal decomposition AHM is a complex process in which several molybdenum compounds are involved. Chithambararaj et al. [28] found that ammonium was still present in the crystalline structures at calcination temperatures up to about 300 °C. According to these authors, at relatively low temperatures AHM evolves from $[NH_4]_4(Mo_8O_{24.8}(O_2)_{1.2}(H_2O)_2)(H_2O)_4$ at 50–75 °C to $[NH_4]_8Mo_{10}O_{34}$ between 100 °C and 200 °C; finally, $[NH_4]_4Mo_8O_{26}$ is formed near 300 °C. Then, $MoO_{2.5}(OH)_{0.5}$ is present between 325 and 475 °C that evolves to $MoO_{2.69}(OH)_{0.3}$ at ca. 575 °C, finally resulting MoO_{3-x} at about 700 °C. It should be noted that molybdenum trioxide can exist both as layered orthorhombic α-MoO_3 and monoclinic β-MoO_3 which has monoclinic rutile type structure formed by edge-sharing MoO_6 octahedra [29]. The XRD patterns of Mo (300), Mo (500) and Mo (700) show also an evolution as the calcination temperature increases. In the case of Mo (700), a mixture of crystalline phases is present that apparently contains MoO_3 and $MoO_{2.69}(OH)_{0.3}$. On the other hand, Mo (500) seems to contain both $MoO_{2.5}(OH)_{0.5}$ and $MoO_{2.69}(OH)_{0.3}$. As for the Mo (300) sample, in addition to $MoO_{2.5}(OH)_{0.5}$ and $MoO_{2.69}(OH)_{0.3}$, the presence of compounds containing ammonium cannot be ruled out.
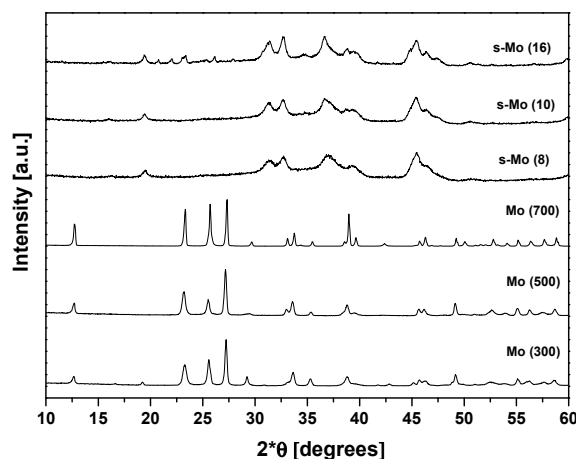

Figure 1. X-ray diffraction (XRD) patterns of the bulk molybdenum catalysts (Mo) calcined at 300, 500, and 700 °C, and of the alumina-supported ones (s-Mo) containing 8, 10 and 16 wt.% MoO_3 and calcined at 800 °C.

In the case of the supported catalysts (calcined at 800 °C), no crystalline molybdenum compound could be identified in the XRD patterns of the samples containing less than 16 wt.% MoO_3 which suggests that the supported species are very well dispersed over the alumina support. However, new diffraction peaks appeared between 20 and 26° (2θ) in the XRD pattern of the s-Mo (16) sample that could correspond to aluminum molybdate ($Al_2(MoO_4)_3$) and to a series of polyoxo Mo species, as reported in the literature for 16 wt.% MoO_3 supported on alumina and calcined at different temperatures between 527 and 827 °C [26]. Kitano et al. [30] investigated a series of alumina-supported

molybdenum catalysts calcined at 800 °C containing between 5 and 30 wt.% MoO_3. No XRD peaks corresponding to Mo compounds were found in the diffraction patterns of the catalysts with MoO_3 loadings below 11 wt.% whereas for contents above 13 wt.% $Al_2(MoO_4)_3$ could be detected. The authors estimated at 10 wt.% the MoO_3 loading required to form a surface monolayer. It was proposed that two-dimensional molybdenum oxide domains and some three-dimensional MoO_3 clusters were formed on 11 wt.% MoO_3/Al_2O_3 whereas the MoO_3 clusters were transformed into aluminum molybdate at higher metallic contents. As can be seen, the XRD results reveal a complex nature of the Mo catalysts that is due to the rich chemistry of this metal.

As expected for the bulk catalysts, these solids showed low specific surface areas that decreased from 17.0 m^2/g for Mo (300) to 4.9 m^2/g for Mo (500) and finally 1.6 m^2/g for Mo (700) as the AHM calcination temperature increased. As for the supported catalysts, their specific surface areas (S_{BET}) are compiled in Table 1; all the samples, included the support, were calcined at 800 °C.

Table 1. Physicochemical characterization data of the supported MoO_3 catalysts.

Sample	S_{BET} (m^2/g)	$[NH_3]_{des.}$ (μmol/m^2) [1]
Al_2O_3 support	112	2.7
s-Mo (6)	99	2.8
s-Mo (8)	72	2.4
s-Mo (10)	63	2.4
s-Mo (13)	47	1.9
s-Mo (16)	44	2.0

[1] Data obtained from the desorption peak centered at 147–150 °C in all cases.

It can be seen that a gradual decrease of the S_{BET} takes place as the MoO_3 loading increases up to 13 wt.%. However, the additional decrease of specific surface area taking place upon an additional MoO_3 loading increase up to 16 wt.% is low resulting in a S_{BET} of 44 m^2/g for s-Mo (16), which represents a decrease of 60% with respect to the alumina support. This indicates a considerable blockage of the porous network, which is not accompanied by the formation of detectable Mo crystalline phases until a 16 wt.% MoO_3 loading is reached, as evidenced by the XRD results. Following the calculations performed by Kitano et al. [30], who assigned a cross-sectional area of 0.22 nm^2 to the octahedral MoO_6 unit, the molybdenum oxide required to form a monolayer over the alumina support used in this work can be estimated at about 11 wt.%. Taking into account these results it could be suggested that in the s-Mo (6) to s-Mo (13) series of samples, Mo oxide seems to be present mainly in the form of a two-dimensional structure well dispersed over the support surface.

The X-ray photoelectron spectroscopy (XPS) results of the bulk molybdenum catalysts are shown in Figure 2.
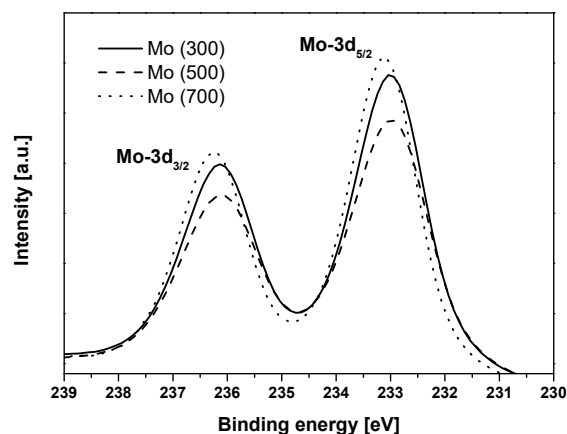

Figure 2. X-ray photoelectron spectra of the Mo 3d doublet corresponding to the bulk MoO_3 catalysts.

In all cases, the XP spectra are characterized by two well-resolved contributions at binding energies of 233.0–233.1 and 236.2–236.3 eV that can be assigned to the Mo $3d_{5/2}$ and Mo $3d_{3/2}$ spin-orbit components of Mo (VI), respectively. The splitting energy of this doublet (3.2 eV) agrees well with the values reported in the literature for Mo (VI) [31]. The presence of molybdenum in oxidation states other than Mo (VI) seems to be not significant though corresponding $3d_{5/2}$ spectral lines have been reported at significantly lower binding energy values (231.6 eV for Mo (V)) [32]. Choi and Thompson indicated values for the Mo $3d_{5/2}$ line of polycrystalline MoO_3 between 231.6 and 232.7 eV [31]. Baltrusaitis et al. [29] compiled a series of values for Mo (VI) taken from the literature and the binding energies reported were 233.0–233.2 eV (Mo $3d_{5/2}$) and 236.1–236.3 eV (Mo $3d_{3/2}$), which coincide with the values found in this work. These values were measured for a layer of oxide thermally developed on molybdenum metal under controlled O_2 pressure [33] as well as for alumina-supported cobalt-molybdena catalysts [34].

Regarding acidity, it was first measured through temperature-programmed desorption of NH_3 (NH_3-TPD), a technique that is not capable of distinguishing between Brönsted and Lewis sites due to the strong basicity of ammonia. As a matter of fact, NH_3 can adsorb on both Lewis and Brönsted sites of MoO_3 as molecular NH_3 and ammonium ion, respectively, though adsorption on Lewis sites is more favorable energetically [35]. The NH_3-TPD patterns corresponding to the alumina support and a selection of the alumina-supported catalysts are included in Figure 3.
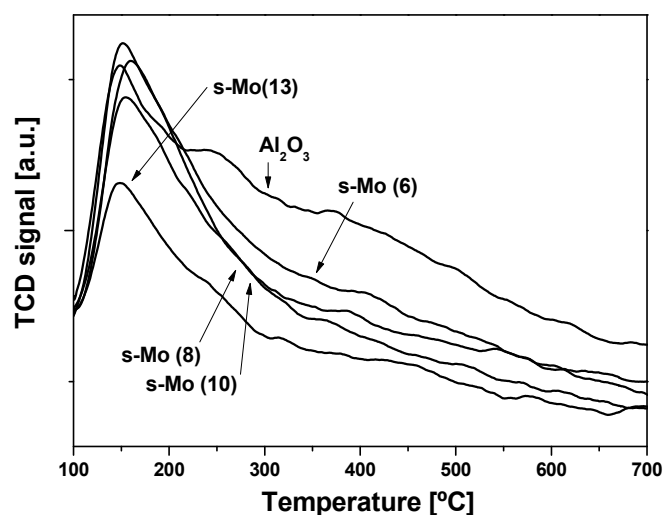

Figure 3. Temperature-programmed desorption of NH_3 (NH_3-TPD) patterns of the samples indicated.

A main peak showing a maximum within the 147–150 °C temperature range characterizes the patterns. The peaks are broad and show a long tail that extends up to 300–600 °C, depending on the case. Very small peaks centered at about 240 °C and 375 °C can be observed in the alumina NH_3-TPD pattern. It is also apparent that baseline drifting complicated the integration of the peaks, which resulted in the specific acidity values compiled in Table 1. It can be seen that the specific acidity tends to decrease as the molybdenum oxide content increases. This result suggests that the acidity of the solids decreases as the alumina surface becomes covered by molybdenum oxide species. Sankaranarayanan et al. [24] found similar NH_3-TPD results for a series of alumina-supported molybdenum oxide catalysts calcined at 527 °C, 677 °C and 827 °C and containing 8wt.%, 12wt.% and 16 wt.% MoO_3. The acidity of the samples calcined at 827 °C decreased from 3.8 μmol/m^2 for the sample loaded with 8 wt.% MoO_3 to 2.8 μmol/m^2 for the catalyst containing 16 wt.% MoO_3. This last result can be compared with the value of 2.0 μmol/m^2 obtained in this work for a sample containing 16 wt.% MoO_3 and calcined at 800 °C (see Table 1). Accurate assessment of the acidity of the unsupported solids through NH_3-TPD was difficult due to the low specific surface area of these materials and the technical limitations of the equipment used (see Section 3) to load high amounts of sample. Their specific acidity was somewhat lower than

that of the supported solids, ranging between 0.6 μmol/m^2 for Mo (300) and 2.0 μmol/m^2 for Mo (500) and Mo (700).

Representative FTIR spectra of adsorbed pyridine corresponding to bulk (Mo (500)) and Al$_2$O$_3$-supported catalysts (s-Mo (8)) are shown in Figure 4. Pyridinium ions adsorbed over Brönsted sites exhibit characteristic bands at wavenumbers of 1546–1548 cm^{-1} (ν_{19b}), and 1638–1640 cm^{-1} (ν_{8a}) [36,37]. The spectra of Mo (500) and s-Mo (8) show weak and broad bands at 1634 and 1638 cm^{-1} as well as at 1532 and 1542 cm^{-1}, respectively. These bands are ascribed to Brönsted sites that due to their different nature appear at different wavenumbers. As for the Lewis sites on molybdenum oxide, bands of adsorbed pyridine at 1451 (ν_{19b}) and 1611 cm^{-1} (ν_{8a}) have been reported [37]. These values are similar to the ones reported for adsorbed pyridine on Al^{3+} in alumina surface: 1450 and 1615 cm^{-1} [36]. The spectrum of the alumina-supported catalyst shows a weak band at 1616 cm^{-1} and another very intense absorption signal at 1442 cm^{-1} that seems compatible with pyridine adsorption on acidic Lewis sites. In the case of the bulk molybdenum oxide catalyst, the band at 1443 cm^{-1} is much weaker and the broad band observed at a wavelength of 1606 cm^{-1} could correspond to the one reported at 1611 cm^{-1} [37]. This difference in intensity indicates a lower number of Lewis sites on the surface of Mo(500) catalyst. Moreover, the position of the band corresponding to the (ν_{8a}) vibration mode of pyridine adsorbed on Lewis sites is used as an indicator of the Lewis strength. Comparing spectra in Figure 4, we can conclude that acidic Lewis sites are stronger in the supported catalyst (1616 cm^{-1} compared to 1606 cm^{-1} in the Mo(500)) [38]. It is interesting to stress that an intense band at 1594 cm^{-1}, absent in the Mo(500) spectrum, is detected in the supported catalyst after pyridine adsorption. This band may be ascribed to species formed by interaction of the probe molecule via N-atom with a weakly acidic H from the surface (denoted as HPy) [39]. Therefore, the new Brönsted sites (unable to protonate pyridine) appear on the supported catalyst, probably due to the interaction of MoO$_3$ with the alumina. It is concluded that both, bulk and supported molybdenum oxide catalysts, have Brönsted and Lewis acid sites, though they are much more abundant and stronger in the case of the supported solids, which is logical due to the presence of the alumina support. Moreover, new Brönsted sites are detected in the supported solid that are not present in the unsupported one.
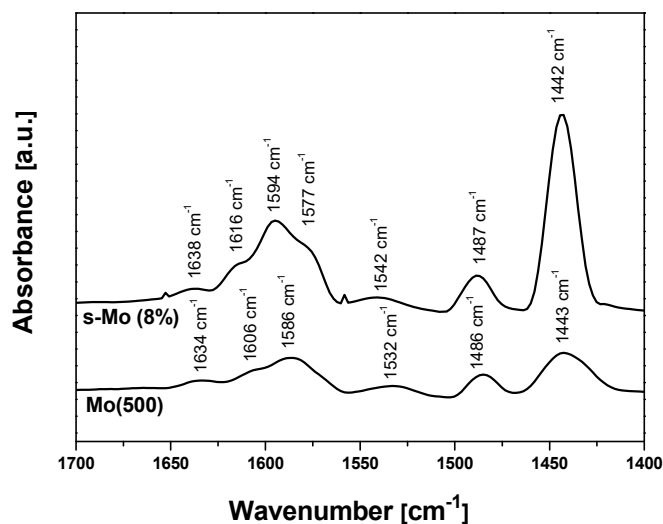

Figure 4. FTIR spectra of adsorbed pyridine on Mo (500) and s-Mo (8) catalysts.

2.2. Catalytic Performance

Figure 5 shows the evolution of the conversion of triglycerides (X$_{TG}$) and FFAs (X$_{FFA}$) with reaction time for the unsupported Mo (300), Mo (500), and Mo (700) catalysts.
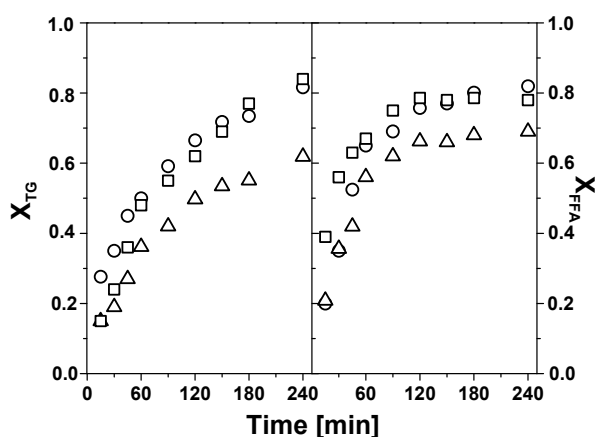
Figure 5. Conversion of the triglycerides (X_{TG}) and FFAs (X_{FFA}) with reaction time for the unsupported Mo (300) (squares), Mo (500) (circles), and Mo (700) (triangles) catalysts. Reaction conditions: 100 °C, 30 atm, methanol/feedstock molar ratio of 12:1, 2 wt.% catalyst referred to the feedstock mass. Feedstock: refined sunflower oil containing 5 wt.% free oleic acid.

It can be seen that both triglycerides and FFAs reach high degrees of conversion (between about 60 and 80%) after 240 min of reaction under the conditions indicated (see Figure 5 caption). The conversion over Mo (300) and Mo (500) are similar, about 80–85% and 78–82% for the triglycerides and FFAs, respectively, after 240 min of reaction. The conversion over Mo (700) is lower, about 60% (triglycerides) and 70% (FFAs) compared to its counterparts calcined at lower temperatures. As the catalyst concentration is fixed on a mass basis (2 wt.%) it is likely that the main cause of these results is the large decrease of the specific surface area experienced by Mo (700) upon calcination. It is also noteworthy that, irrespective of the catalyst used, X_{TG} gradually increases with reaction time, whereas FFAs conversion shows a faster initial increase until about 120 min of reaction, with a much slower increase taking place afterward.

Regarding the yields of the several reaction products, Figure 6a shows the evolution with X_{TG} of the diglycerides (Y_{DG}), monoglycerides (Y_{MG}), and methyl esters produced by transesterification ($Y_{ME,trans.}$) (see Equations (3)–(5) in Section 3).

The evolution of the products yields is in accordance with the scheme of the triglycerides (TG) methanolysis reaction consisting of three consecutive steps [4]. In the first step, a molecule of TG is converted into a diglyceride (DG), which then evolves to a monoglyceride (MG) that finally gives glycerol. In each step, a molecule of methanol is consumed and a methyl ester (biodiesel) molecule is formed. This explains why initially, at low X_{TG}, DG were clearly the most abundant products. As the conversion increases, Y_{DG} also increases reaching maximum values of about 35% for X_{TG} within the 60–70% range; then, DG started to decline. The yield of both monoglycerides, and especially methyl esters, increase with the conversion of triglycerides. Maximum biodiesel yields achieved are about 30% and correspond to the highest conversions reached at the end of the catalytic runs (80–85%). It is noteworthy that there are no significant differences among the yields provided by the three unsupported catalysts at similar X_{TG}, meaning that the selectivity is not affected by the calcination temperature of the unsupported catalysts.

Ferreira Pinto et al. [23] reported a maximum FAME yield of 64.2% for an unsupported MoO$_3$ catalyst calcined at 600 °C after 4 h of reaction during the methanolysis of soybean oil acidified with 10 wt.% of oleic acid. Yields were slightly lower (50–56%) for solids calcined at lower temperatures (300–500 °C), and dropped to 43% for MoO$_3$ calcined at 700 °C. This trend is similar to the one observed in our work. Ferreira Pinto et al. [23] performed the catalytic tests at considerably higher temperature (150 °C) and methanol to feedstock molar ratio (30:1) than in this work, being the catalyst concentration also higher (5 wt.%), though the vegetable oil contained double FFAs concentration (10 wt.%). These authors found a correlation between the catalytic activity and the acidity of the solids as determined

through a titration technique in which aqueous NaOH previously contacted with the catalyst was neutralized with HCl. It was suggested that the changes provoked by the thermal treatment affected the acid properties of the catalysts. The lower biodiesel yields found in this work can be mainly attributed to the milder reaction conditions and lower catalyst concentration employed. On the other hand, the slightly higher specific acidity, developed as the calcination temperature increases, is virtually offset by the accompanying specific surface area decrease.
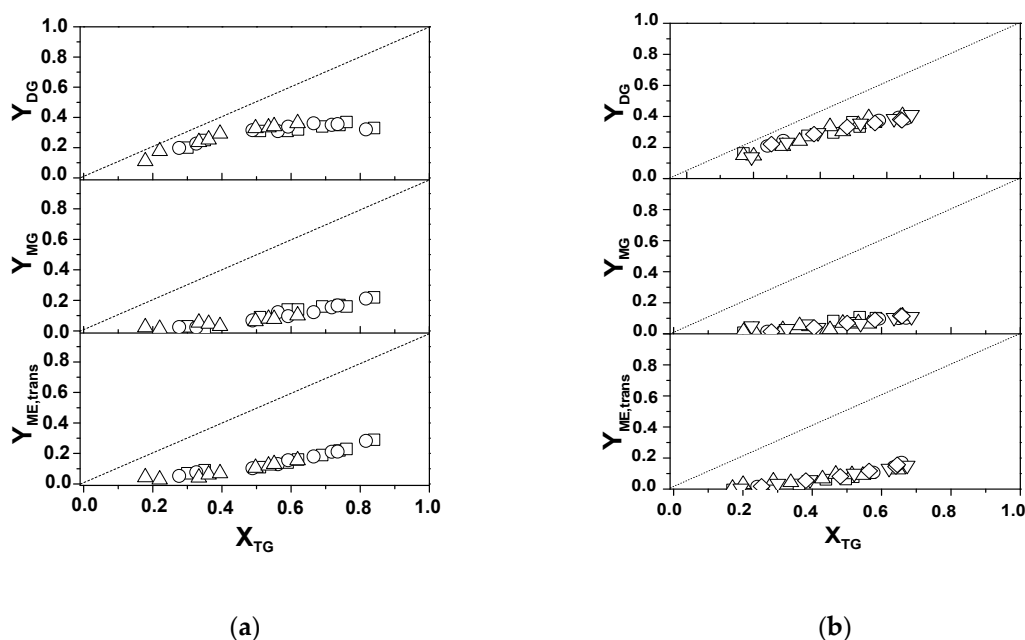

(a)

(b)

Figure 6. Evolution with the triglycerides conversion of the yields of diglycerides (Y_{DG}), monoglycerides (Y_{MG}), and methyl esters produced by transesterification ($Y_{ME,trans.}$) for: (**a**) unsupported Mo (300) (squares), Mo (500) (circles), and Mo (700) (triangles) catalysts; (**b**) supported s-Mo (6) (squares); s-Mo (8) (circles); s-Mo (10) (triangles); s-Mo (13) (inverted triangles); s-Mo (16) (rhombus) catalysts. Reaction conditions: 100 °C, 30 atm, methanol:feedstock molar ratio of 12:1, 2 wt.% catalyst referred to the feedstock mass. Feedstock: refined sunflower oil containing 5 wt.% free oleic acid.

As for the supported solids, Figure 7 shows the conversions of triglycerides and FFAs reached by the alumina-supported catalysts loaded with 6 to 16 wt.% MoO_3. It should be noted that experiments carried out with the alumina support under the same reaction conditions provided negligible transesterification and esterification conversions. It merits to be highlighted that the feedstock conversions provided by the bulk catalysts are much higher than those of the supported ones. In this regard, after 240 min of reaction, X_{TG} and X_{FFA} reach values between 40–60% and 65–75%, respectively, which are significantly lower than the conversions provided by the unsupported catalysts under similar reaction time (see Figure 5). Final conversions after 480 min range between 55% and 75% for X_{TG} and 70–80% for X_{FFA}. Concerning the effect of the MoO_3 oxide content, it seems that the activity goes through a maximum as the molybdenum oxide content increases. Indeed, both transesterification and esterification conversions increase when passing from s-Mo (6) to s-Mo (8) which is the catalyst providing the highest conversions. Then, the conversions decrease for s-Mo (10), s-Mo (13), and s-Mo (16), which reach relatively similar values.

The findings that the alumina support is not active and that the unsupported catalysts are significantly more active than the alumina-supported ones indicate that the catalytic activity is mainly associated with molybdenum oxide species. Nevertheless, a positive effect of the support in dispersing the active phase is also apparent because the MoO_3 contents were as low as 0.12–0.32 wt.% in the case of the supported catalysts compared with 2 wt.% for the unsupported ones. On the other hand, the acidity of the catalyst as determined by NH_3-TPD does not constitute in this case a suitable measure to predict

the activity in the simultaneous transesterification and esterification reactions. This is because alumina showed specific acidities comparable and even higher than those of the supported catalysts (see Table 1). Notwithstanding, additional effects of the MoO_3-Al_2O_3 interactions on the catalytic activity cannot be ruled out; for instance, the presence of Brönsted acid sites of the [=Mo-O(H)-Al=] bridging type, similar to the ones proposed for MoO_3-Al_2O_3 catalytic systems in other works [30,34,37]. These sites could correspond to the adsorbed pyridinium and HPy species detected by FTIR spectroscopy upon pyridine adsorption over the supported catalysts (see previous section). As the specific surface area decreases with the increase of the MoO_3 content (see Table 1), the opposite effects of molybdenum oxide on the textural and certain acidic properties could explain that the catalytic activity within the s-Mo (6) to s-Mo (16) series of catalysts reaches a maximum value for an intermediate MoO_3 content, in this case, 8 wt.%.
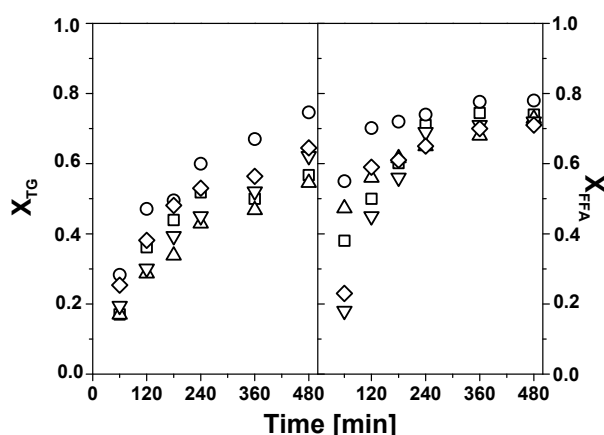

Figure 7. Evolution with reaction time of the conversion of triglycerides (X_{TG}) and FFAs (X_{FFA}) for supported s-Mo (6) (squares); s-Mo (8) (circles); s-Mo (10) (triangles); s-Mo (13) (inverted triangles); s-Mo (16) (rhombus) catalysts. Reaction conditions: 100 °C, 30 atm, methanol/feedstock molar ratio of 12:1, 2 wt.% catalyst referred to the feedstock mass. Feedstock: refined sunflower oil containing 5 wt.% free oleic acid.

Sankaranarayanan et al. [24] found a triglycerides conversion of about 58% (FAME yield of 47%) after 8 h of reaction at 100 °C with methanol to oil molar ratio of 9 using a 16 wt.% MoO_3/Al_2O_3 catalyst calcined at 677 °C at a concentration of 5 wt.%. The feedstock used consisted of refined sunflower oil (non-acidified). This result can be compared with about 64% triglycerides conversion in this work after 8 h of reaction at the same temperature, slightly higher methanol to oil molar ratio (12), but significantly lower concentration (2 wt.%) of the s-Mo (16) catalyst during the methanolysis of sunflower oil acidified with 5 wt.% of FFAs (see Figure 7). As in our case, Sankaranarayanan et al. [24] also found that the alumina support was not active for the transesterification reaction within the 60–110 °C range of temperature. As for the effect of the MoO_3 content of the catalysts, these authors found that it depended on the calcination temperature. In this regard, a large increase of activity was found when passing from 12 to 16 wt.% for catalysts calcined at 527 °C that greatly decreased when the calcination temperature increased to 827 °C; moreover, the catalysts calcined at 677 °C were more active than the ones calcined at 827 °C regardless the MoO_3 content [24]. These results were explained in terms of a higher specific activity of the well-dispersed molybdenum oxide species resulting at relatively low calcination temperatures and the presence of poorly active aluminum molybdate formed at high Mo loadings and calcination temperatures.

The yields of the several products given by the supported catalysts are presented in Figure 6b. It can be seen that there are no significant differences among the solids, meaning that the MoO_3 content does not affect the catalyst selectivity in the transesterification reaction. The yields of methyl esters were significantly lower than the ones reported by Sankaranarayanan et al. [24], though it should be

remembered that these authors used non-acidified refined sunflower oil. The yields of methyl esters and monoglycerides were also lower than the ones obtained with the unsupported catalysts when the results are compared at the same triglycerides conversion, indicating a different performance, which is ascribed to the different nature of the active sites in both types of solids.

2.3. Catalysts Stability

As it is well-known, a key issue in the field of biodiesel production with heterogeneous catalysts is the chemical stability of the solids in the reaction medium, which is directly connected with both the possibility of reutilizing the catalyst and the quality of the produced biodiesel and glycerol, in particular, the fulfillment of the corresponding standards for their typical uses.

In this work, Mo (500) and s-Mo (8) catalysts were recovered after reaction, thoroughly washed with tetrahydrofuran (THF), which is an excellent solvent for the reaction mixture medium [40], calcined at their respective original temperatures (500 °C and 800 °C, respectively), and used again. Mo (500) yielded almost the same catalytic activity results than during its first use. XRD and N_2-adsorption data evidenced that no substantial changes took place during reaction. To check the possible occurrence of molybdenum leaching into the reaction mixture, the Mo (500) catalyst was removed after reaction by centrifugation. The upper fraction was transferred to a rotary evaporator to remove the unreacted methanol, resulting in a liquid that acquired an intense blue color that evidenced the presence of molybdenum. The molybdenum concentration was measured by ICP atomic emission spectroscopy resulting in ca. 1000 ppm of Mo. Additionally, Mo (500) was mixed with methanol for 4 h under the typical conditions used in this work. The solid was removed afterwards by centrifugation and the methanol was used in a reaction run. An X_{TG} value of 75% was obtained after 4 h of reaction, which is only slightly lower than the value of 82% achieved in the presence of the solid catalyst (see Figure 5). Clearly, leached molybdenum species were capable of homogeneously catalyzing the transesterification and esterification reactions. The fact that the recovered solid gives the same feedstock conversion than the fresh catalyst is not strange provided that the solid represents a sufficiently excess amount with respect to its solubility in the reaction medium, thus guaranteeing the activity during several re-utilization cycles. As a matter of fact, it is likely that the concentration of ca. 1000 ppm of Mo measured is close to the solubility limit of the molybdenum species in the polar phase. Ferreira Pinto et al. [23] reutilized unsupported MoO_3 in eight consecutive cycles of acidified soybean oil methanolysis. The catalyst was filtered from run to run and was used without washing. A very low loss of activity was observed only during the two last cycles; however, information about Mo leaching was not provided.

Regarding s-Mo (8), catalyst recovery, washing with THF, calcination, and reuse was repeated four times. The X_{TG} values recorded after 8 h of reaction are shown in Figure 8. A gradual decrease of the triglycerides conversion takes place during the first three reaction cycles. The conversion stabilizes at values about 40% after a fourth reaction cycle; a conversion 47% lower than the original value.

As described before for Mo (500), s-Mo (8) was mixed also with methanol for 4 h under the typical conditions used in this work. When used in a reaction run, the recovered methanol yielded X_{TG} and X_{FFA} values of 41% and 46%, respectively, after 4 h of reaction. These conversions were substantially lower than the 60% and 73% values obtained in the presence of fresh s-Mo (8). Mo leaching after the first reaction cycle was investigated following the procedure described above for the unsupported catalyst. Although the Mo concentration could not be measured, the color of the liquid phase resulting after methanol removal evidenced the presence of dissolved Mo. On the whole, the results point to a somewhat improved stability of the supported catalysts compared to the unsupported ones that could be attributed to the interaction established between MoO_3 and Al_2O_3. This interaction has been evidenced by the XRD results that showed the formation of aluminum molybdate, which seems to contribute to an improved dispersion and anchorage of the molybdenum species. This leads to a comparatively high activity for low MoO_3 loadings and reduced leaching in comparison with the unsupported catalysts.
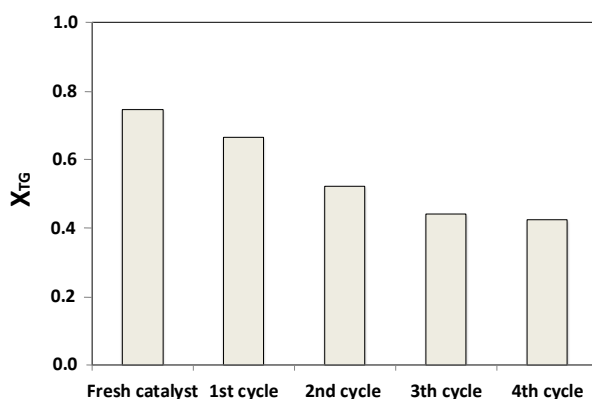
Figure 8. Triglycerides conversion (X_{TG}) obtained after 8 h of reaction during the number of reuse cycles indicated for the catalyst s-Mo (8). Reaction conditions: 100 °C, 30 atm, methanol/feedstock molar ratio of 12:1, 2 wt.% catalyst referred to the feedstock mass. Feedstock: refined sunflower oil containing 5 wt.% free oleic acid.

3. Materials and Methods

MoO_3 was synthesized by thermal decomposition of ammonium heptamolybdate tetrahydrate (AHM, from Merck, Darmstadt, Germany) in air (6 h) using a muffle furnace at different temperatures (300, 500 and 700 °C). The resulting solids were labeled as Mo (300), Mo (500) and Mo (700), respectively. Supported molybdenum catalysts were prepared by incipient wetness impregnation of $\gamma-Al_2O_3$ (Spheralite 505, Procatalyse) in powder form (particle size between 100 and 200 μm) previously calcined at 800 °C (6 h) in order to remove adsorbed impurities. Different impregnating AHM aqueous solutions were prepared to adjust the Mo salt concentration in order to obtain several MoO_3 contents in the final catalyst, namely 6, 8, 10, 13 and 16 wt.%. After impregnation, the solids were dried for 8 h at 80 °C and calcined for 6 h at 800 °C in a muffle furnace. The calcination temperature was selected in order to promote the interaction of molybdenum species with the alumina support with the aim of improving their resistance to leaching during the reaction. The supported catalysts were referred to as s-Mo followed by the corresponding nominal MoO_3 content between parentheses.

As for the catalysts characterization, XRD analyses were carried out in a D-Max Rigaku diffractometer (Akishima-shi, Tokyo, Japan). Specific surface areas were measured through N_2 adsorption at −196 °C using a Micromeritics Gemini V 2380 apparatus (Norcross (Atlanta), GA, USA). Acidity was characterized by NH_3-TPD in a Micromeritics Autochem 2920 equipment (Norcross (Atlanta), GA, USA). Pyridine adsorption was carried out using a purpose-made quartz IR cell connected to a vacuum adsorption device with a residual pressure lower than 10^{-4} Pa. The samples, in the form of wafers, were activated and pyridine introduced into the cell at room temperature. Spectra were recorded in a Thermo Nicolet 380 spectrophotometer (Waltham, MA, USA) with a DTGS/KBr detector (Waltham, MA, USA) and accumulating 128 scans at a spectral resolution of 4 cm^{-1}. X-ray photoelectron spectroscopy (XPS) analyses were carried out on a SPECS system equipped with an Al anode XR50 source operating at 150 W and a Phoibos 150 MCD-9 detector (Berlin, Germany). The pass energy of the hemispherical analyzer was set at 25 eV and the energy step was set at 0.1 eV. Charge stabilization was achieved by using a SPECS Flood Gun FG 15/40. The sample powders were pressed to self-consistent disks. Data processing was performed with the CasaXPS program (Casa Software Ltd., Teignmouth, UK).

Catalytic tests were carried out in batch mode in a Parr 4843 stainless steel autoclave reactor with mechanical stirring under controlled temperature and pressure. The feedstock consisted of refined sunflower oil (Urzante, Navarra, Spain; Acid Value of 0.07 mg KOH/g) to which pure oleic acid (Sigma Aldrich, San Luis, MO, USA) was added until it reached an FFAs content of 5 wt.% (Acid Value of 10.0 mg KOH/g). Catalyst concentration was set at a relatively low value of 2 wt.% referred to the feedstock (oil and FFAs mixture) mass. Simultaneous esterification of FFAs and transesterification

of the triglycerides (TG) with methanol (Scharlau, HPLC grade, Barcelona, Spain) was carried out at 100 °C and methanol/feedstock molar ratio of 12:1. The amounts of the several substances used were: sunflower oil 60 g, FFAs 3 g, catalyst 1.26 g, and methanol 27.5 g. After reaching the reaction temperature, the reactor was pressurized with nitrogen until reaching an absolute pressure of 30 atm. Samples withdrawn from the reactor were analyzed by size exclusion chromatography as described elsewhere [40]. Conversion of triglycerides (X_{TG}) and free fatty acids (X_{FFA}), and yields of diglycerides (Y_{DG}), monoglycerides (Y_{MG}), and methyl esters (FAMEs) produced by transesterification ($Y_{ME,trans.}$) were calculated through Equations (1)–(5), respectively:

$$X_{TG} = \frac{N_{TG,0} - N_{TG}}{N_{TG,0}} \tag{1}$$

$$X_{FFA} = \frac{N_{FFA,0} - N_{FFA}}{N_{FFA,0}} \tag{2}$$

$$Y_{DG} = \frac{N_{DG}}{N_{TG,0}} \tag{3}$$

$$Y_{MG} = \frac{N_{MG}}{N_{TG,0}} \tag{4}$$

$$Y_{ME,trans.} = \frac{N_{ME} - (N_{FFA,0} \cdot X_{FFA})}{N_{TG,0}}, \tag{5}$$

where $N_{TG,0}$ and $N_{FFA,0}$ stand for the initial number of moles of triglycerides and FFAs, respectively, and N_{TG}, N_{DG}, N_{MG}, N_{ME}, and N_{FFA} stand for the number of moles of triglycerides, diglycerides, monoglycerides, FAMEs and FFAs, respectively, present in a sample taken at a given reaction time. Note that in Equation (5), in order to calculate the yield of methyl esters produced by transesterification, the number of moles of methyl esters produced by the esterification of FFAs ($N_{FFA,0} \cdot X_{FFA}$) is subtracted from the total number of methyl esters present in the sample.

4. Conclusions

The MoO$_3$-Al$_2$O$_3$ catalytic system has provided positive results consisting of high triglycerides conversions into biodiesel under conditions of high FFAs content that would have made the conventional transesterification reaction impossible in a single step with basic catalysts. Moreover, the FFAs are efficiently converted into biodiesel as well. Compared to bulk MoO$_3$, alumina-supported MoO$_3$ leads to a more efficient utilization of the active phase and enhanced stability towards molybdenum leaching by the reaction medium. These effects likely arise from the interaction established between MoO$_3$ and alumina that affect the textural and acidic properties of the catalysts. However, much effort is still required to develop a sufficiently stable catalyst based on molybdenum oxide for transforming triglycerides with high FFAs content into biodiesel.

Author Contributions: All the authors participated actively in the writing and editing of the manuscript. Furthermore: conceptualization, A.N. and L.M.G.; methodology, A.N.; catalysts preparation, textural and structural characterization, and catalytic testing, A.N. and I.R.; acid properties characterization, E.J.-B. and F.R.-S.; XPS characterization J.L.; results interpretation and discussion, and literature review, all the authors; project administration and funding acquisition, L.M.G. All authors have read and agreed to the published version of the manuscript.

References

1. Mittelbach, M. Fuels from oils and Fats: Recent developments and perspectives. *Eur. J. Lipid Sci. Technol.* **2015**, *117*, 1832–1846. [CrossRef]

2. Chhetri, A.B.; Watts, K.C.; Islam, M.R. Waste Cooking Oil as an Alternate Feedstock for Biodiesel Production. *Energies* **2008**, *1*, 3–18. [CrossRef]

3. Navajas, A.; Issariyakul, T.; Arzamendi, G.; Gandía, L.M.; Dalai, A.K. Development of eggshell derived catalyst for transesterification of used cooking oil for biodiesel production. *Asia-Pac. J. Chem. Eng.* **2013**, *8*, 742–748. [CrossRef]

4. Arzamendi, G.; Campo, I.; Arguiñarena, E.; Sánchez, M.; Montes, M.; Gandía, L.M. Synthesis of biodiesel with heterogeneous NaOH/alumina catalysts: Comparison with homogeneous NaOH. *Chem. Eng. J.* **2007**, *134*, 123–130. [CrossRef]

5. Navajas, A.; Campo, I.; Arzamendi, G.; Hernández, W.Y.; Bobadilla, L.F.; Centeno, M.A.; Odriozola, J.A.; Gandía, L.M. Synthesis of biodiesel from the methanolysis of sunflower oil using PURAL® Mg–Al hydrotalcites as catalyst precursors. *Appl. Catal. B Environ.* **2010**, *100*, 299–309. [CrossRef]

6. Reyero, I.; Bimbela, F.; Navajas, A.; Arzamendi, G.; Gandía, L.M. Issues concerning the use of renewable Ca-based solids as transesterification catalysts. *Fuel* **2015**, *158*, 558–564. [CrossRef]

7. Reyero, I.; Moral, A.; Bimbela, F.; Radosevic, J.; Sanz, O.; Montes, M.; Gandía, L.M. Metallic monolithic catalysts based on calcium and cerium for the production of biodiesel. *Fuel* **2016**, *182*, 668–676. [CrossRef]

8. Lotero, E.; Liu, Y.; Lopez, D.E.; Suwannakarn, K.; Bruce, D.A.; Goodwin, J.G., Jr. Synthesis of Biodiesel via Acid Catalysis. *Ind. Eng. Chem. Res.* **2005**, *44*, 5353–5363. [CrossRef]

9. Tesser, R.; Di Serio, M.; Guida, M.; Nastasi, M.; Santacesaria, E. Kinetics of oleic acid esterification with methanol in the presence of triglycerides. *Ind. Eng. Chem. Res.* **2005**, *44*, 7978–7982. [CrossRef]

10. Di Serio, M.; Tesser, R.; Pengmei, L.; Santacesaria, E. Heterogeneous Catalysts for Biodiesel Production. *Energy Fuels* **2008**, *22*, 207–217. [CrossRef]

11. Melero, J.A.; Iglesias, J.; Morales, G. Heterogeneous acid catalysts for biodiesel production: Current status and future challenges. *Green Chem.* **2009**, *11*, 1285–1308. [CrossRef]

12. Sreeprasanth, P.S.; Srivastava, R.; Srinivas, D.; Ratnasamy, P. Hydrophobic, solid acid catalysts for production of biofuels and lubricants. *Appl. Catal. A: Gen.* **2006**, *314*, 148–159. [CrossRef]

13. Thanh, L.T.; Okitsu, K.; Boi, L.V.; Maeda, Y. Catalytic Technologies for Biodiesel Fuel Production and Utilization of Glycerol: A Review. *Catalysts* **2012**, *2*, 191–222. [CrossRef]

14. Su, F.; Guo, Y. Advancements in solid acid catalysts for biodiesel production. *Green Chem.* **2014**, *16*, 2934–2957. [CrossRef]

15. Sani, Y.M.; Daud, W.M.A.W.; Aziz, A.R.A. Activity of solid acid catalysts for biodiesel production: A critical review. *Appl. Catal. A: Gen.* **2014**, *470*, 140–161. [CrossRef]

16. Gupta, P.; Paul, S. Solid acids: Green alternatives for acid catalysis. *Catal. Today* **2014**, *236*, 153–170. [CrossRef]

17. Mansir, N.; Taufiq-Yap, Y.H.; Rashid, U.; Lokman, I.M. Investigation of heterogeneous solid acid catalyst performance on low grade feedstocks for biodiesel production: A review. *Energ. Convers. Manag.* **2017**, *141*, 171–182. [CrossRef]

18. Hanif, M.A.; Nisar, S.; Rashid, U. Supported solid and heteropoly acid catalyst for production of biodiesel. *Catal. Rev.* **2017**, *59*, 165–188. [CrossRef]

19. Park, Y.-M.; Chung, S.-H.; Eom, H.J.; Lee, J.-S.; Lee, K.Y. Tungsten oxide zirconia as solid superacid catalyst for esterification of waste acid oil (dark oil). *Bioresour. Technol.* **2010**, *101*, 6589–6593. [CrossRef]

20. Kaur, M.; Malhotra, R.; Ali, A. Tungsten supported Ti/SiO$_2$ nanoflowers as reusable heterogeneous catalyst for biodiesel production. *Renew. Energ.* **2018**, *116*, 109–119. [CrossRef]

21. Haber, J. Molybdenum Compounds in Heterogeneous Catalysis. In *Molybdenum: An Outline of its Chemistry and Uses*; Braithwaite, E.R., Haber, J., Eds.; Elsevier: Amsterdam, The Netherlands, 1994; Chapter 10; pp. 477–617.

22. Nakagaki, S.; Bail, A.; dos Santos, V.C.; Rodrigues de Souza, V.H.; Vrubel, H.; Souza Nunes, F.; Pereira Ramos, L. Use of anhydrous sodium molybdate as an efficient heterogeneous catalyst for soybean oil methanolysis. *Appl. Catal. A: Gen.* **2008**, *351*, 267–274. [CrossRef]

23. Ferreira Pinto, B.; Suller Garcia, M.S.; Santos Costa, J.C.; Rodarte de Moura, C.V.; Chaves de Abreu, W.; Miranda de Moura, E. Effect of calcination temperature on the application of molybdenum trioxide acid catalyst: Screening of substrates for biodiesel production. *Fuel* **2019**, *239*, 290–296. [CrossRef]

24. Sankaranarayanan, T.M.; Pandurangan, A.; Banu, M.; Sivansanker, S. Transesterification of sunflower oil over MoO_3 supported on alumina. *Appl. Catal. A: Gen.* **2011**, *409–410*, 239–247. [CrossRef]

25. Bail, A.; dos Santos, V.C.; Roque de Freitas, M.; Pereira Ramos, L.; Schreiner, W.H.; Ricci, G.P.; Ciuffi, K.J.; Nakagaki, S. Investigation of a molybdenum-containing silica catalyst synthesized by the sol-gel process in heterogeneous catalytic esterification reactions using methanol and ethanol. *Appl. Catal. B: Environ.* **2013**, *130–131*, 314–324. [CrossRef]

26. Sankaranarayanan, T.M.; Thirunavukkarasu, K.; Banu, M.; Pandurangan, K.; Sivansanker, S. Activity of supported MoO_3 catalysts for the transesterification of sunflower oil. *Int. J. Adv. Eng. Sci. Appl. Math.* **2013**, *5*, 197–209. [CrossRef]

27. Mouat, A.R.; Lohr, T.L.; Wegener, E.C.; Miller, J.T.; Delferro, M.; Stair, P.C.; Marks, T.J. Reactivity of a carbon-supported single-site molybdenum dioxo catalyst for biodiesel synthesis. *ACS Catal.* **2016**, *6*, 6762–6769. [CrossRef]

28. Chithambararaj, A.; Bhagya Mathi, D.; Rajeswari Yogamalar, N.; Chandra Bose, A. Structural evolution and phase transition of $[NH_4]_6Mo_7O_{24.4}H_2O$ to 2D layered MoO_{3-x}. *Mater. Res. Express* **2015**, *2*, 055004. [CrossRef]

29. Baltrusaitis, J.; Mendoza-Sanchez, B.; Fernandez, V.; Veenstra, R.; Dukstiene, N.; Roberts, A.; Fairley, N. Generalized molybdenum oxide surface chemical state XPS determination via informed amorphous sample model. *Appl. Surf. Sci.* **2015**, *326*, 151–161. [CrossRef]

30. Kitano, T.; Okazaki, S.; Shishido, T.; Teramura, K.; Tanaka, T. Brønsted acid generation of alumina-supported molybdenum oxide calcined at high temperatures: Characterization by acid-catalyzed reactions and spectroscopic methods. *J. Mol. Catal. A: Chem.* **2013**, *371*, 21–28. [CrossRef]

31. Choi, J.-G.; Thompson, L.T. XPS study of as-prepared and reduced molybdenum oxides. *Appl. Surf. Sci.* **1996**, *93*, 143–149. [CrossRef]

32. Deng, X.; Ying Quek, S.; Biener, M.M.; Biener, J.; Hyuk Kang, D.; Schalek, R.; Kaxiras, E.; Friend, C.M. Selective thermal reduction of single-layer MoO_3 nanostructures on Au(111). *Surf. Sci.* **2008**, *602*, 1166–1174. [CrossRef]

33. Światowska-Mrowiecka, J.; de Diesbach, S.; Maurice, V.; Zanna, S.; Klein, L.; Briand, E.; Vickridge, I.; Marcus, P. Li-Ion Intercalation in Thermal Oxide Thin Films of MoO_3 as Studied by XPS, RBS, and NRA. *J. Phys. Chem. C* **2008**, *112*, 11050–11058. [CrossRef]

34. Patterson, T.A.; Carver, J.C.; Leyden, D.E.; Hercules, D.M. A surface study of cobalt-molybdena-alumina catalyst using X-Ray Photoelectron Spectroscopy. *J. Phys. Chem.* **1976**, *80*, 1700–1708. [CrossRef]

35. Yan, Z.; Fan, J.; Zuo, Z.; Li, Z.; Zhang, J. NH_3 adsorption on the Lewis and Bronsted acid sites of MoO_3 (010) surface: A cluster DFT study. *Appl. Surf. Sci.* **2014**, *288*, 690–694. [CrossRef]

36. Morterra, C.; Magnacca, G. A case study: Surface chemistry and surface structure of catalytic aluminas, as studied by vibrational spectroscopy of adsorbed species. *Catal. Today* **1996**, *27*, 497–532. [CrossRef]

37. Skara, G.; Baran, R.; Onfroy, T.; De Proft, F.; Dzwigaj, S.; Tielens, F. Characterization of zeolitic intraframework molybdenum sites. *Micropor. Mesopor. Mater.* **2016**, *225*, 355–364. [CrossRef]

38. Bagshaw, S.A.; Cooney, R.P. FTIR Surface Site Analysis of Pillared Clays Using Pyridine Probe Species. *Chem. Mater.* **1993**, *5*, 1101–1109. [CrossRef]

39. Penkova, A.; Bobadilla, L.F.; Romero-Sarria, F.; Centeno, M.A.; Odriozola, J.A. Pyridine adsorption on NiSn/MgO–Al_2O_3: An FTIR spectroscopic study of surface acidity. *Appl. Surf. Sci.* **2014**, *317*, 241–251. [CrossRef]

40. Arzamendi, G.; Arguiñarena, E.; Campo, I.; Gandía, L.M. Monitoring of biodiesel production: Simultaneous analysis of the transesterification products using size-exclusion chromatography. *Chem. Eng. J.* **2006**, *122*, 31–40. [CrossRef]